Cerebral Cortex
Regular Article

Dysfunction of KCNK Potassium Channels Impairs Neuronal Migration in the Developing Mouse Cerebral Cortex

A brief title: KCNK Dysfunction Impairs Cortical Development

Yuki Bando[1, 2], Tomoo Hirano[1], and Yoshiaki Tagawa[1, 2]

[1]Department of Biophysics, Kyoto University Graduate School of Science,

Kitashirakawa-Oiwake-cho, Sakyo-ku, Kyoto 606-8502, Japan

[2]CREST, Japan Science and Technology Agency, Kawaguchi, Saitama 332-0012, Japan

Correspondence should be addressed to Y.T. (tagawa@neurosci.biophys.kyoto-u.ac.jp)

Department of Biophysics, Kyoto University Graduate School of Science,

Kitashirakawa-Oiwake-cho, Sakyo-ku, Kyoto 606-8502, Japan

Tel: +81-75-753-4238

Fax: +81-75-753-4229

Total number of pages, 42

Figures, 8

Word counts: Abstract, 200 words

Key words: activity dependent, calcium, channelopathy, electroporation, mental retardation

Abstract

Development of the cerebral cortex depends partly on neural activity, but the identity of the ion channels that might contribute to the activity-dependent cortical development is unknown. KCNK channels are critical determinants of neuronal excitability in the mature cerebral cortex, and a member of the KCNK family, KCNK9, is responsible for a maternally transmitted mental retardation syndrome. Here, we have investigated the roles of KCNK family potassium channels in cortical development. Knockdown of KCNK2, 9, or 10 by RNAi using *in utero* electroporation impaired the migration of late-born cortical excitatory neurons destined to become layer II/III neurons. The migration defect caused by KCNK9 knockdown was rescued by coexpression of RNAi-resistant functional KCNK9 mutant. Furthermore, expression of dominant-negative mutant KCNK9, responsible for the disease, and electrophysiological experiments demonstrated that ion channel function was involved in the migration defect. Calcium imaging revealed that KCNK9 knockdown or expression of dominant-negative mutant KCNK9 increased the fraction of neurons showing calcium transients and the frequency of spontaneous calcium transients. Mislocated neurons seen after KCNK9 knockdown stayed in the deep cortical layers, showing delayed morphological maturation. Taken together, our results suggest that dysfunction of KCNK9 causes a migration defect in the cortex via an activity-dependent mechanism.

Introduction

Neural activity plays roles in the formation of neural circuits (Katz and Shatz, 1996). In addition to its well-documented role in the refinement of circuits, some studies have shown that neural activity is also required for early neuronal development, including proliferation (Weissman et al., 2004; Liu et al., 2010), differentiation (Borodinsky et al., 2004), and migration (Komuro and Rakic, 1993; Nakanishi and Okazawa, 2006; Manent and Represa, 2007; Bortone and Polleux, 2009). In the developing cerebral cortex of rodents, studies using extracellular recording and calcium imaging have demonstrated that the immature cortical neurons show characteristic patterns of activity (Khazipov and Luhmann, 2006; Allene and Cossart, 2010). Such activity is thought to influence cortical development. Hypo- or hyper-activity during development may induce abnormality in the cortical architecture, which might be the basis for some developmental disorders (Ross and Walsh, 2001; Ben-Ari, 2008). These roles of neural activity in multiple developmental stages suggest that controlling neuronal activity is vital for the proper development of immature neurons.

The pattern of neural activity is regulated by ion channels. Developing cortical neurons express various ion channels, such as voltage-gated sodium channels, potassium channels, and calcium channels (Luhmann et al., 2000; Picken Bahrey and Moody, 2003). KCNK family leak potassium channels, which have four trans-membrane segments and two P-domains, are one of the major determinants of membrane potential (Goldstein et al., 2001). They conduct potassium current at resting membrane potential with little voltage-dependence, and are therefore called leak potassium channels.

KCNK channels are critical determinants of neuronal excitability in the cortex (Goldstein et al., 2001; Day et al., 2005). In addition, a member of the KCNK family, KCNK9 (TASK3), is responsible for a maternally transmitted developmental disorder, Birk Barel mental retardation dysmorphism syndrome (Barel et al., 2008), and KCNK9 knockout mice show abnormalities in some cognitive functions such as working memory and spatial learning (Linden et al., 2007). Several members of the KCNK family (KCNK9, KCNK2/TREK1 and KCNK10/TREK2) are expressed in the developing cerebral cortex (Talley et al., 2001; Aller and Wisden, 2008). These facts imply that KCNK9 is involved in cortical function, and might also be involved in the formation of cortical neural circuits. However, whether dysfunction of KCNK9 affects cortical development has not yet been explored. In this study, we addressed this issue, and found that knockdown of KCNK9 expression by RNAi affected migration of cortical neurons. Functional blockade of KCNK9 by overexpression of a dominant-negative, disease-associated mutant channel (Barel et al., 2008) also disturbed this migration. KCNK9 knockdown neurons showed more frequent calcium transients than control neurons. These results suggest that KCNK potassium channels contribute to the migration of cortical pyramidal neurons through stabilization of intracellular calcium concentration.

Material and Methods

Animals

Wild-type ICR mice were used in all experiments. The experimental procedures were

performed in accordance with the guidance for animal experimentation by the United States National Institutes of Health and Kyoto University, and were approved by the local committee for handling experimental animals in the Graduate School of Science, Kyoto University.

Plasmid construction

KCNK2, 9, and 10 shRNAs were obtained from Open Biosystems. Each shRNA was inserted into a pCAGmir30 vector (Matsuda and Cepko, 2007). The sequences of KCNK9 shRNA2 and 3 were designed using the Hannon lab web site (http://cancan.cshl.edu/RNAi_central/main2.cgi), and were inserted into a pSuper vector under the H1 promoter (OligoEngine). The sequences of shRNAs used in this study are shown in Supplementary Table S1. The numbers of shRNAs initially obtained were 1 for KCNK2, 4 for KCNK9, and 1 for KCNK10. One KCNK9 shRNA did not effectively reduce the expression of KCNK9 protein in HEK293T cells, and therefore was not used for futher experiments. Mouse cDNA encoding KCNK9 was isolated from a cDNA library of adult mouse cortex by polymerase chain reaction. Mouse cDNAs encoding KCNK2 and 10 were purchased from Open Biosystems. Mutant and N-terminal EGFP-tagged KCNK channels were cloned into a pCAGplay vector (Kawaguchi and Hirano, 2006). For western blot, EGFP was fused to N-terminus of each KCNK channel with a linker (Gly-Ser-Ala). The pCAsalEGFP vector (Horikawa and Takeichi, 2001) was used for expression of enhanced green fluorescent protein (EGFP). GCaMP3 cDNA was purchased from Addgene (plasmid 22692), and inserted into pCAGplay vector. The

sequences of primers used to obtain mutant and EGFP-tagged KCNK channels are shown in Supplementary Table S3.

In situ *hybridization.*

In situ hybridization was performed as previously described (Tagawa et al., 2005; Watakabe et al., 2007). KCNK2, 9, and 10 cDNAs were cut by restriction enzymes (KCNK2, BamHI/HincII; KCNK9, PstI; KCNK10, BamHI/PstI), and subcloned into pBluescript. Digoxogenin (DIG)-labeled RNA probes were transcribed by T3 or T7 RNA polymerases. Embryonic and neonatal mouse brains were cryoprotected in OCT compound (Sakura), and coronal sections of 20 μm were cut on a cryostat CM1850 (Leica). The sections were fixed with 4 % paraformaldehyde for 10 min at room temperature, followed by washing twice in 2x SSC for 3 min at room temperature. The sections were incubated with 0.1 M triethanolamine for 3 min, and then acetic anhydride was added and the sections were incubated for 10 min at room temperature. The sections were hybridized with DIG-labeled RNA probes for 40 hr at 65 ℃ in hybridization solution (50 % formamide, 5x SSC, 5x Denhardt's solution, 50 ng/ml yeast tRNA), followed by washing with 2x SSC for 30 min at 65 ℃, 0.5x SSC for 15 min at 65 ℃ and 0.5x SSC for 15 min at room temperature. The sections were incubated with alkaline phosphatase-conjugated anti-DIG (Roche) at 4 ℃ overnight. The hybridization signal was detected with TSA-plus Fluorescein System (Perkin Elmer) for 10 min at room temperature. The sections were mounted with Vectashield containing DAPI (Vector).

In utero *electroporation*

In utero electroporation was performed as reported previously (Saito and Nakatsuji, 2001; Tabata and Nakajima, 2001; Mizuno et al., 2007). In brief, ICR mice at E15 were anesthetized with Somnopentyl (50 mg/kg, Kyoritsu Pharmacy), and their uteruses were exposed. Plasmid vectors were prepared at 0.2 mg/ml (KCNK9*, G95E, G95E*, G236R, G236R*), 0.5 mg/ml (GCaMP3) or 1.0 mg/ml (others) with Trypan Blue (Sigma), and 1 ~ 2 μl DNA solution was injected into the right lateral ventricle. Next, five electric pulses of 50 V for 50 ms at 1 Hz were applied to the embryos using an electroporator CUY21EDIT (NepaGene).

Immunohistochemistry

Neonatal (P0 ~ 5) and juvenile (P10, 15 and 35) mice were deeply anesthetized. Brains were fixed with 4 % paraformaldehyde in phosphate buffer at 4 ℃ overnight, transferred to 30 % sucrose in phosphate buffered saline (PBS), and incubated at 4 ℃ overnight. Neonatal brains were cryoprotected in OCT compound (Sakura), and coronal sections of 50 μm were cut on a cryostat CM1850 (Leica). Fifty-micrometer-thick coronal sections of juvenile brains were cut on a freezing microtome LM2000R (Leica).

Immunohistochemistry was performed using a free-floating procedure. The sections were incubated with blocking solution (5 % normal goat serum (Sigma), 0.2 % Triton X-100 in PBS) for 1 hr at room temperature, followed by incubation with primary antibodies in blocking solution at 4 ℃ overnight. Subsequently, the sections were

incubated with secondary antibodies for 1 hr at room temperature. The sections were mounted with Vectashield containing DAPI (Vector). The following primary and secondary antibodies were used: anti-GFP (chick, polyclonal, 1:600, Millipore), anti-Cux1 (rabbit, polyclonal, 1:100, Santa Cruz Biotechnology), Ctip2 (rat, monoclonal, 1:600, Abcam), anti-Tbr1 (rabbit, polyclonal, 1:600, Abcam), anti-Ki67 (rabbit, monoclonal, 1:1000, Thermo Scientific), anti-Nestin (mouse, monoclonal, 1:600, BD Pharmingen), anti-KCNK3 (1 mg/ml, Alomone Labs), Alexa 488-conjugated anti-chick IgG, Alexa 568-conjugated anti-rabbit IgG, anti-mouse IgG, and anti-rat IgG (made in goat, 1:1000, Molecular Probes).

Detection of apoptosis with TUNEL assay

Apoptosis was detected with an ApopTag® Red *In Situ* Apoptosis Detection Kit (Chemicon). The experimental procedure was based on the protocol that was provided by the manufacturer. Briefly, 50-μm-thick coronal cortical sections were incubated with ethanol/acetic acid for 5 min at room temperature. Sections were incubated with TdT enzyme and DIG-labeled dNTP for 30 min at 37 ℃. Subsequently, sections were incubated with rhodamine-conjugated anti-DIG antibody for 30 min at room temperature. Finally, sections were mounted with Vectashield containing DAPI (Vector).

Microscopy and morphological analysis

Fluorescent images were acquired on a confocal laser-scanning microscope FV1000

(Olympus). For acquisition of images of *in situ* hybridization and analysis of neuronal migration, a 10x dry objective was used. Images of a single confocal plane were acquired for *in situ* hybridization. Confocal images of 50-μm-thick z-stacks were acquired for analysis of neuronal migration, and the z-series of images were projected onto two dimensional representations. The fraction of EGFP-positive neurons in each layer was calculated by dividing the number of EGFP-positive neurons in each cortical layer by that of total EGFP-positive neurons in the cortex. At least 10 sections (one section per mouse) for each experimental condition were analyzed.

For acquisition of images to analyze the cell fate, proliferation, apoptosis and dendritic morphology, a 20x dry objective was used. Images of a single confocal plane were acquired for analysis of cell fate, proliferation and apoptisis, and z-series of images were obtained for morphological analysis. Z-series of images were projected onto two-dimensional planes. Dendrites were traced, and total length and branch points were analyzed with NeuronJ software (Meijering et al., 2004) (http://rsb.info.nih.gov/ij/). At least 5 neurons from one mouse were analyzed.

Statistical analysis was performed with Student's t-test or the Dunnett test. All results were expressed as mean ± SEM.

Western blotting

Plasmids encoding EGFP-tagged KCNK2, 9, 10, KCNK9*, G95E* or G236R* with or without shRNA expression vectors (2 μg for each) were transfected into HEK293T cells with Lipofectamine 2000 (Invitrogen), based on the protocol that was provided by the

manufacturer. Twenty-four hours after transfection, the cells were lysed in sample loading buffer (50 mM Tris-HCl, 4 % SDS, 20 % glycerol, 10 mM dithiothreitol, 0.001 % bromophenol blue), and were denatured for 30 minutes at 37 ℃. The samples were separated by 10 % SDS-PAGE, and transferred onto nitrocellulose membranes. The membranes were incubated with blocking solution (5 % skim milk and 0.1 % Tween-20 in TBS) for 1 hour at room temperature, and incubated with primary antibody (mouse monoclonal anti-GFP, 1:1000, Nacalai Tesque; mouse monoclonal anti-β-actin, 1:1000, Sigma) in blocking solution overnight at 4 ℃. The membranes were incubated with HRP-conjugated secondary antibody (donkey monoclonal anti-mouse IgG, 1:1000, Molecular Probes) in TBS for 1 hour at room temperature. Signals were detected with an ECL Chemiluminescent kit (GE Healthcare). Images were acquired using LAS 3000 (Fuji Film).

Electrophysiology

Electrophysiological experiments were performed as previously described (Ohtsuki et al, 2004). In brief, neonatal mouse brains were removed, and coronal 300 μm thick cortical slices were cut on a vibratome (linear slicer PRO 7, Dosaka EM) in chilled RDS solution (130 (mM) NaCl, 4.5 KCl, 2 $CaCl_2$, 33 glucose and 5 HEPES). Slices were recovered for longer than 1 hour in Krebs' solution saturated with 95 % O_2 and 5% CO_2 (124 (mM) NaCl, 26 $NaHCO_3$, 1.8 KCl, 1.24 KH_2PO_4, 2.5 $CaCl_2$, 1.3 $MgCl_2$ and 10 glucose) at room temperature. Oxygenized Krebs' solution was used as extracellular bath solution. The glass patch pipettes of 4 ~ 7 MΩ were used for recording. The patch pipettes were filled

with the internal solution (140 (mM) D-glucuronic acid, 7 KCl, 155 KOH, 5 EGTA, 10 HEPES, 2 Mg-ATP and 0.2 Na-GTP). The junction potential was offset. Whole-cell recordings from migrating neurons in intermediate zone of P1 cortex were performed at room temperature (22 ~ 24 ℃) with a patch clamp amplifier (EPC 9 or 10, HEKA). In voltage clamp experiments, the membrane potential was held at -60 mV. Input resistance was measured by applying -20 mV voltage pulses, and voltage-dependent inward and outward currents were recorded by applying positive voltage pulses with a 10 mV step. Resting potential was recorded in a current clamp condition. Statistical analysis was performed with Student's t-test. All results were expressed as mean ± SEM.

Calcium imaging

GCaMP3 cDNA with control, KCNK9 shRNA, or KCNK9 G236R were transfected by *in utero* electroporation. Coronal 500-μm-thick cortical slices of P1 mice were cut on a vibratome in chilled RDS solution. Slices were allowed to recover for longer than 1 hour in Krebs' solution saturated with 95 % O_2 and 5% CO_2 at room temperature. Krebs' solution was used as extracellular solution. Optical recording was performed at room temperature, using a fluorescent microscope BX50WI (Olympus) with a 20x water-immersion objective and an EM-CCD camera C9100 (Hamamatsu Photonics). The sampling rate was 1 Hz. The mean fluorescent signal of a single cell was calculated, and divided by that at the start using Aquacosmos software (Hamamatsu Photonics). A fluorescence change of 5 % above the baseline within 30 sec was regarded as a calcium

transient. Statistical analysis was performed with the χ^2-test or Dunnett test. All results were expressed as mean ± SEM.

Results

Expression pattern of KCNK potassium channels in developing cortex

Previous studies showed the expression of KCNK2, KCNK9 and KCNK10 in the developing cortex (Aller and Wisden, 2008), but their laminar distributions were unclear. As a first step to study the roles of KCNK potassium channels in cortical development, we examined the expression patterns of these potassium channels in the developing cortex by *in situ* hybridization.

[Figure 1 here]

KCNK2 was expressed in the cortical plate (CP), intermediate zone (IZ), subventricular zone (SVZ) and ventricular zone (VZ) at embryonic day 15 (E15) and E17. At postnatal day 0 (P0), KCNK2 was strongly expressed in the marginal zone (MZ), IZ, SVZ, VZ, and lower CP, but not in upper CP. It was expressed in layers I, V and VI, but was not expressed in layers II/III or IV at P3 (Fig. 1*A*). KCNK9 was expressed in MZ, CP, IZ, SVZ and VZ at E15 and 17. At P0 and 3, KCNK9 was expressed in all cortical layers except layer I. The expression level of KCNK9 in CP increased after birth (Fig. 1*B*). KCNK10 was most highly expressed at E15. KCNK10 was strongly expressed in MZ, IZ, SVZ and VZ, and was weakly expressed in CP. At P0, KCNK10 was expressed in MZ, lower CP, IZ, SVZ and VZ. KCNK10 was weakly expressed in the lower cortical layers at P3 (Fig. 1*C*). Taken together, these findings indicate that KCNK2, 9, and 10

were expressed in SVZ and VZ at E15, and in IZ, SVZ and VZ at E17 and P0, suggesting that developing cortical neurons, including layer II/III neurons, express these KCNK potassium channels in the late embryonic and early postnatal stages.

Neuronal migration was impaired by knockdown of KCNK potassium channels

To determine whether KCNK potassium channels are involved in the cortical development, we performed RNAi experiments using *in utero* electroporation. Short hairpin RNAs (shRNAs) targeting KCNK2, 9 and 10 effectively inhibited the expression of each KCNK channel protein in HEK293T cells, whereas control shRNA did not affect the translation of mRNAs for these genes (Fig. 2*A*). A mutant variant of KCNK9 shRNA was used as a control shRNA (Supplementary Table S1).

[Figure 2 here]

The control or KCNK channel shRNA was then transfected into cortical layer II/III progenitor cells together with EGFP. Coronal cortical sections including visual, auditory, or somatosensory cortices were prepared at P0, 3 and 5, and the distribution of EGFP-positive neurons was examined. At P0, about half of EGFP- and control shRNA-expressing neurons were observed in IZ, SVZ, and VZ, and some EGFP-positive neurons were observed in the upper CP. The distributions of EGFP-positive neurons were not altered by knockdown of KCNK channels at P0 (Fig. 2*B,C*, Supplementary Table S2). Most neurons expressing control shRNA had arrived at the superficial layer by P3 (Fig. 2*B,C*, Supplementary Table S2, 83.4 ± 5.1 %, n = 11 sections). In contrast,

only a fraction of neurons expressing KCNK channel shRNAs reached layer II/III at P3 (Fig. 2*B*,*C*, Supplementary Table S2, KCNK2 shRNA, 40.7 ± 2.3 %, n = 11, P < 0.001, Dunnett test; KCNK9 shRNA, 24.5 ± 2.1 %, n = 10, P < 0.001; KCNK10 shRNA, 47.7 ± 4.5 %, n = 11, P < 0.001). A decrease in the fraction of neurons in IZ/SVZ/VZ between P0 and P3 was small in KCNK knockdown mice (Fig. 2*B*,*C*, Supplementary Table S2, control shRNA P0, 52.3 ± 2.7 %, n = 12; P3, 10.1 ± 3.6 %, n = 11; KCNK2 shRNA P0, 50.3 ± 3.0 %, n = 11; P3, 41.9 ± 2.3 %, n = 11; KCNK9 shRNA P0, 46.2 ± 2.1 %, n = 11; P3, 47.1 ± 4.3 %, n = 10; KCNK10 shRNA P0, 47.5 ± 1.5 %, n = 12; P3, 39.8 ± 3.8 %, n = 11), suggesting that an invasion into the cortical plate was decelerated by knockdown of KCNK channels. At P5, some neurons expressing KCNK9 shRNA still remained in deep cortical layers (Fig. 2*B*,*C*, Supplementary Table S2, Control shRNA, 3.6 ± 1.3 %, n = 14; KCNK2 shRNA, 1.9 ± 0.6 %, n = 12, P = 0.698, Dunnett test; KCNK9 shRNA, 9.8 ± 1.8 %, n = 10, P = 0.002; KCNK10 shRNA, 2.3 ± 1.1 %, n = 12, P = 0.858) and white matter (Fig. 2*B*,*C*, Supplementary Table S2, Control shRNA, 10.4 ± 3.7 %, n = 14; KCNK2 shRNA, 8.3 ± 3.1 %, n = 12, P = 0.977, Dunnett test; KCNK9 shRNA , 38.0 ± 2.3 %, n = 10, P < 0.001; KCNK10 shRNA, 8.2 ± 2.7 %, n = 12, P = 0.975), but most EGFP-positive neurons expressing KCNK2 or 10 shRNA had reached superficial layer (Fig. 2*B*,*C*, Supplementary Table S2, Control shRNA, 86.0 ± 4.6 %, n = 14; KCNK2 shRNA, 89.9 ± 3.5 %, n = 12, P = 0.872, Dunnett test; KCNK9 shRNA 52.2 ± 2.4 %, n = 10, P < 0.001; KCNK10 shRNA, 89.5 ± 2.6 %, n = 12, P = 0.906). Thus, knockdown of KCNK2, 9 or 10 impaired neuronal migration at P3, but only KCNK9 knockdown significantly impaired neuronal migration at P5. Knockdown of

these three members of KCNKs (KCNK2, 9 and 10) together impaired neuronal migration as severely as KCNK9 knockdown (Fig. 2*B,C*, Supplementary Table S2, P5, Layer II/III, 54.8 ± 4.2 %, $P < 0.001$; Layers IV-VI, 13.8 ± 1.7 %, $P < 0.001$; WM, 31.5 ± 4.4 %, $P < 0.001$, compared with control shRNA, n = 14). These results suggest that KCNK family leak potassium channels are involved in the migration of cortical layer II/III neurons. We focused on the function of KCNK9 in neuronal migration and performed further analysis of it, because knockdown of KCNK9 most clearly impaired neuronal migration.

[Figure 3 here]

Ion channel function of KCNK9 was required for neuronal migration

We next confirmed that the impairment of migration by KCNK9 shRNA expression was not caused by an off-target effect. Two other shRNAs for KCNK9, whose target sequences were different from that of KCNK9 shRNA, also inhibited the expression of KCNK9 (Fig. 3*A*). These shRNAs impaired neuronal migration, like KCNK9 shRNA (Fig. 3*B,C*, Supplementary Table S2, layer II/III, pSuper, 94.1 ± 1.3 %, n = 12 sections; KCNK9 shRNA2, 18.3 ± 1.4 %, n = 11, $P < 0.001$, Dunnett test; KCNK9 shRNA3, 28.8 ± 1.6 %, n = 11, $P < 0.001$). Next, we attempted to rescue the phenotype by expressing mutant KCNK that was resistant to shRNA. We introduced mutations that disrupted the target sequence of KCNK9 shRNA but that did not alter the amino acid sequence. Indeed, the expression of this mutant KCNK9 (KCNK9*) was not inhibited by KCNK9 shRNA (Fig. 3*D*). The impairment of neuronal migration was partially rescued by

co-expression of KCNK9* with KCNK9 shRNA (KCNK9 rescue) at P3 (Fig. 3*E,F*, Supplementary Table S2, Layer II/III, KCNK9 shRNA, 35.9 ± 2.7 %, n = 11 sections; KCNK9 rescue, 65.4 ± 3.0 %, n = 11, $P < 0.001$, Dunnett test). These results suggest that the impairment of neuronal migration was caused by knockdown of KCNK9.

[Figure 4 here]

To examine further the role of KCNK9 in neuronal migration, we used two KCNK9 mutant channels. Previous studies showed that glycine 95 at the potassium-selective filter and glycine 236 at the ion channel pore are crucial for the ion channel function of KCNK9. The mutants G95E and G236R are nonfunctional when expressed alone, and act as dominant-negative proteins when expressed with the wild-type channel (Pei et al., 2003; Barel et al., 2008) (Fig. 4*A*). We performed electroporation with these mutant channels. Neuronal migration was impaired at P3 by the expression of these dominant-negative mutants (Fig. 4*B,C*, Supplementary Table S2, Layer II/III, EGFP, 84.6 ± 3.6 %, n = 10; G95E, 54.6 ± 3.4 %, n = 12, $P < 0.001$, Dunnett test; G236R, 38.5 ± 1.1 %, n = 11, $P < 0.001$). This result supported our findings from RNAi experiments and suggested that the expression and/or function of KCNK9 were critical for neuronal migration.

The crucial role of channel function of KCNK9 in the migration was suggested by another set of experiments. As mentioned above, migration defect caused by KCNK9 knockdown could be rescued by coexpression of RNAi-resistant functional KCNK9 (KCNK9*) channel (Fig. 3*E,F*, Supplementary Table S2). However, migration defect caused by KCNK9 knockdown was not recovered by coexpression of RNAi-insensitive

nonfunctional G95E or G236R mutant (Fig. 4*E*,*F*, Supplementary Table S2). Thus, the ion channel function of KCNK9 is necessary for the normal neuronal migration.

[Figure 5 here]

The requirement for ion channel function of KCNK9 for neuronal migration suggests that knockdown of KCNK9 might have altered electrophysiological properties of migrating neurons. It was shown that KCNK9 is critically involved in the regulation of resting membrane potential in cerebellar granule neurons (Brickley et al., 2007). We performed whole-cell patch-clamp recording from migrating cortical neurons expressing control shRNA or KCNK9 shRNA. Knockdown of KCNK9 significantly increased input resistance (Fig. 5*A*,*B*, control shRNA, 3.3 ± 0.7 GΩ, n = 16 neurons; KCNK9 shRNA, 9.7 ± 2.0 GΩ, n = 17 neurons, P = 0.004, Student's t-test). KCNK9 knockdown also significantly depolarized the resting membrane potential (Fig. 5*C*, control shRNA, -58.2 ± 5.1 mV, n = 16 neurons; KCNK9 shRNA, -40.9 ± 3.1 mV, n = 17 neurons, P = 0.007, Student's t-test). On the other hand, KCNK9 knockdown did not affect the voltage-dependent transient inward current (control shRNA, -90.1 ± 24.6 pA, n = 16 neurons; KCNK9 shRNA, -91.8 ± 21.3 pA, n = 17 neurons at -10 mV, P = 0.960, Student's t-test) or sustained outward current (control shRNA, 197 ± 27.8 pA, n = 16 neurons; KCNK9 shRNA, 159 ± 11.2 pA, n = 17 neurons at 0 mV, P = 0.227, Student's t-test) induced by depolarizing voltage steps (Fig. 5*D*-*F*). These results are consistent with the known roles of KCNK channels (Goldstein et al., 2001) and suggest that KCNK9 contributes to the resting potassium permeability of membranes in migrating cortical neurons.

[Figure 6 here]

Down-regulation of KCNK9 increased the frequency of spontaneous calcium transients

Neuronal migration is partly regulated by intracellular calcium (Zheng and Poo, 2007). We thought that KCNK9 knockdown or functional blockade might alter the pattern of spontaneous calcium transients. To test this, we transfected a genetically encoded calcium indicator, GCaMP3 (Tian et al., 2009), with control, KCNK9 shRNA or a dominant-negative mutant, G236R, and performed calcium imaging from migrating neurons at P0/P1 (Fig. 6). A small fraction (about 10 %) of neurons expressing control shRNA showed calcium transients at a frequency of about 1 event/10min (Fig. 6*A*,*B*). We compared the pattern of spontaneous calcium transients between control and KCNK9 knockdown neurons in both IZ and lower CP. The fraction of neurons expressing KCNK9 shRNA that showed calcium transients was more than that of control neurons at P1 (P0 IZ, control shRNA, 7.1 %, 18/254 neurons; KCNK9 shRNA, 11.7 %, 15/128 neurons, $P = 0.128$, χ^2-test; P0 lower CP, control shRNA, 10.7 %, 15/140 neurons; KCNK9 shRNA, 12.6 %, 27/214 neurons, $P = 0.588$; P1 IZ, control shRNA, 11.0 %, 19/173 neurons; KCNK9 shRNA, 25.5 %, 39/153 neurons, $P < 0.001$; P1 lower CP, control shRNA, 9.2 %, 7/76 neurons; KCNK9 shRNA, 25.2 %, 37/147 neurons, $P = 0.005$). At P0, the frequency of spontaneous calcium transients in KCNK9 knockdown neurons was higher than that in control neurons in IZ, but not in lower CP (Fig. 6*A*,*B,* IZ, control shRNA, 1.2 ± 0.1 events/10 min, n = 18 neurons; KCNK9 shRNA, 2.7 ± 0.7 events/10

min, n = 15 neurons, P = 0.024, Student's t-test; lower CP, control shRNA, 1.3 ± 0.1 events/10 min, n = 15 neurons; KCNK9 shRNA, 1.6 ± 0.2 events/10 min, n = 27 neurons, P = 0.191). At P1, the frequency of spontaneous calcium transients in KCNK9 knockdown neurons was higher than that in control neurons both in IZ and lower CP (Fig. 6*A*,*B,* IZ, control shRNA, 1.3 ± 0.1 events/10 min, n = 19 neurons; KCNK9 shRNA, 2.9 ± 0.5 events/10 min, n = 39 neurons, P = 0.002; lower CP, control shRNA, 1.1 ± 0.1 events/10 min, n = 7 neurons; KCNK9 shRNA, 2.1 ± 0.2 events/10 min, n = 37 neurons, P = 0.001, Student's t-test). Thus, KCNK9 knockdown increased the frequency of spontaneous calcium transients in migrating cortical neurons.

Is there any correlation between an increase in calcium transients and the migration defect? To test this, we carried out another set of experiments in which we compared the pattern of calcium transients in neurons expressing control shRNA, KCNK9 shRNA, or KCNK9 shRNA with RNAi-insensitive KCNK9 (KCNK9*) (Fig. 6*C*,*D*). The increase in the frequency of calcium transients caused by KCNK9 knockdown was partially "rescued" by coexpression of KCNK9* (Fig. 6*C*,*D*, KCNK9 rescue, fraction of neurons, 47/138 neurons; frequency, 2.0 ± 0.2 events/10 min, n = 47 neurons, P = 0.012, compared with KCNK9 shRNA, P = 0.471, compared with control shRNA, Dunnett test). Thus, coexpression of RNAi-insensitive KCNK9 with KCNK9 shRNA partially restored both the pattern of calcium transients (Fig. 6*C*,*D*) and the migration phenotype (Fig. 3*E*,*F*).

We also examined effects of the expression of a disease-associated, dominant-negative mutant (G236R) of KCNK9. The fraction of neurons showing

calcium transients was significantly higher in dominant-negative mutant transfected mice (GCaMP3, 4.7%, 13/279 neurons, G236R, 33.9 %, 57/168 neurons, $P < 0.001$, χ^2-test). Furthermore, the frequency of calcium transients was higher in neurons expressing G236R than in control neurons showing calcium transients (Fig. 6*E,F*, GCaMP3, 1.4 ± 0.2 events/10min, n = 13 neurons, G236R, 3.1 ± 0.3 events/10min, n = 57 neurons, $P < 0.001$, Student's t-test). These results together suggest that dysfunction of KCNK9 influences the pattern of calcium transients in migrating neurons.

Cell fate, neuronal proliferation, and apoptosis were not affected by knockdown of KCNK9

Next we performed immunohistochemistry to examine whether the cell fate of neurons that failed to migrate was changed or not. Previous studies identified several genes expressed in a layer-specific manner, and some genes have been reported to be determinants of the neuronal subtype specification in the cerebral cortex (Molyneaux et al., 2007). Tbr1 is a determinant of corticothalamic neurons in layer VI, and preplate (Hevner et al., 2001). Ctip2 promotes the differentiation of layer V corticospinal motor neurons (Arlotta et al., 2005). Cux1 is expressed in layers II/III and IV, but is not expressed in the other layers (Nieto et al., 2004).

[Figure 7 here]

Coronal cortical sections were stained with antibodies against Cux1, Ctip2 or Tbr1. Neurons expressing EGFP and control shRNA were Cux1-positive, consistent with

previous studies (Fig. 7*A*). KCNK9 shRNA-expressing neurons that reached layer II/III were also Cux1-positive (Fig. 7*B*). KCNK9 shRNA-expressing neurons that failed to migrate also expressed Cux1, but did not express Ctip2 or Tbr1 (Fig.7*B*). These results suggest that cell fate specification is not affected by KCNK9 knockdown.

Previous studies have shown a role of KCNK9 in the development of cerebellar granule neurons, in which this channel is highly expressed (Talley et al., 2001; Han et al., 2002) and involved in potassium-dependent apoptosis (Lauritzen et al., 2003). In addition, KCNK9 has been implicated in cell division in tumor cells (Mu et al., 2003; Pei et al., 2003). We performed immunostaining against Ki67, which is a marker for cell division, and TUNEL staining for detection of apoptotic cells at E17. The fraction of EGFP/Ki67-double-positive cells (Fig. 7*C,D*, control shRNA, 9.3 ± 1.2 %; KCNK9 shRNA, 10.2 ± 1.9%, n = 12 sections for each, P = 0.691, Student's t-test) and the number of TUNEL-positive cells (Fig. 7*E,F*, control shRNA, 5.3 ± 0.7 cells; KCNK9 shRNA, 5.6± 0.8 cells, n = 12 sections for each, P = 0.755, Student's t-test) were not significantly different between control and KCNK9 shRNA (Fig. 7*C-F*). In addition, immunostaining against Nestin showed that radial glial scaffold was not affected by KCNK9 knockdown (Fig. 7*G*). These results suggest that knockdown of KCNK9 does not affect neuronal proliferation, apoptosis and radial glial scaffold.

[Figure 8 here]

KCNK9 knockdown impeded morphological maturation

What is the fate of neurons showing a migration defect during the neonatal period? Do

they stay in deep cortical layers and mature, or eventually disappear? To answer these questions, we examined the laminar distribution of EGFP-positive neurons expressing KCNK9 shRNA at P10, 15 and 35. At P35, the fraction of EGFP-positive neurons in WM was slightly smaller than that at P10 (Fig. 8*A*,*B*, Supplementary Table S2, P10, 12.1 ± 1.8 %, n = 11 sections; P15, 8.7 ± 2.0 %, n = 15, P = 0.322, Dunnett test: P35, 4.1 ± 1.3 %, n = 10, P = 0.014), but the fraction of EGFP-positive neurons in layer II/III and layers IV-VI did not significantly differ among these ages (Fig. 8*A*,*B*, Supplementary Table S2, layer II/III, P10, 77.9 ± 2.7 %, n = 11; P15, 80.7 ± 2.4 %, n = 15, P = 0.635, Dunnett test; P35, 83.6 ± 2.4 %, n = 10, P = 0.243, layers IV-VI, P10, 10.0 ± 1.4 %; P15, 10.6 ± 1.1 %, P = 0.926; P35, 12.6 ± 1.3 %, P = 0.291). At P35, some of neurons in WM may have moved into the cortex, not have died, because the number of EGFP-positive cells did not significantly change among ages (P10, 146.0 ± 20.0 neurons; P15, 133.0 ± 10.7 neurons P = 0.786, Dunnett test; P35, 152.5 ± 20.1 neurons, P = 0.948). These results suggest that many of the mislocated neurons resulting from KCNK9 knockdown stay in deep cortical layers during development. At P10, many EGFP-positive neurons in deep cortical layers had apical protrusions with few branches, reminiscent of the leading process of typical migrating neurons (Fig. 8*C*,*F*,*G*, branch points, 1.2 ± 0.3; total length, 287.3 ± 25.7 μm, n = 34 neurons). At P15, these neurons had some branched dendrites (Fig. 8*D*,*F*,*G*, branch points, 3.3 ± 0.7, P = 0.019, Dunnett test; total length, 384.7 ± 42.5 μm, P = 0.348, n = 23 neurons), and at P35, they had complex dendritic arbors, similar to those of mature neurons (Fig. 8*E*-*G*, branch points, 10.9 ± 0.8, P < 0.001; total length, 2081.0 ± 133.0 μm, P < 0.001,

n = 27 neurons). These observations suggest that dendritic maturation is delayed in neurons that failed to migrate due to KCNK9 knockdown, and that these neurons somehow mature by P35 in deep cortical layers.

Discussion

We have demonstrated that KCNK potassium channels, especially KCNK9, play an important role in neuronal migration in the developing cerebral cortex. Knockdown of KCNK9 in late-born cortical neurons by RNAi resulted in a migration defect. Expression of the dominant-negative mutant channel G236R, found in patients with an inherited mental retardation (Barel et al., 2008), also caused a migration defect in the cortex, suggesting that ion channel function is required for neuronal migration. Electrophysiological experiments showed that knockdown of KCNK9 depolarize resting membrane potential. Knockdown or functional blockade of KCNK9 with the dominant-negative mutant channel G236R increased the frequency of spontaneous calcium transients. Taken together, these results suggest that dysfunction of KCNK9 impairs migration of cortical excitatory neurons in an activity-dependent mechanism.

Dysfunction of KCNK9 can cause a migration defect in the cortex

Our data, obtained from RNAi experiments using three independent shRNAs, rescue experiments, and functional blockade experiments using dominant-negative mutants, indicate that a deficit in the expression/function of KCNK9 can cause a migration defect in the cortex. Earlier studies reported that KCNK9 knockout mice showed abnormality

in some cognitive functions and in the regulation of cellular excitability in mature cerebellar granule neurons (Brickley et al., 2007; Linden et al., 2007). It is unclear whether migration of cortical excitatory neurons is impaired in KCNK9 knockout mice, because these studies did not focus on neuronal migration in the cortex. There are several cases where the extent of migration defects caused by genetic knockout is not comparable to that by *in utero* knockdown (Bai et al., 2003; Chen et al., 2008; Ip et al., 2011), and in the genetic knockout mice, compensatory mechanisms by other family members have been suggested (Corbo et al., 2002; Deuel et al., 2006; Koizumi et al., 2006). *In utero* knockdown can be a useful approach for identifying genetic factors responsible for abnormality in cortical development, and for further investigation on how loss-of-function of target molecules affects cortical neuron development.

Developing cortical neurons express several members of KCNK potassium channels (Aller and Wisden, 2008). When one of these (e.g. KCNK9) is knocked down, other members (e.g. KCNK2 and/or 10) may compensate for the reduced expression. However, we did not observe an additive effect of multiple knockdown: the distribution of EGFP-positive neurons in KCNK2/9/10 knockdown cortex was comparable to that in single knockdown of KCNK9 at P0, 3 and 5 (Fig. 2*B*, *C*, Supplementary Table S2). KCNK9 may play a dominant role in neuronal migration in the developing cortex.

It is reported that KCNK3 (TASK1) can form heterodimer with KCNK9 in cerebellar granule cells and motoneurons and modulate its ion channel function (Berg et al., 2004, Kang et al., 2004). There is a possibility that KCNK3 may be involved in KCNK9-dependent regulation of neuronal migration in the developing cerebral cortex.

However, a previous report has shown no or low expression of KCNK3 mRNA in the developing cerebral cortex (Aller and Wisden, 2008). Our immunohistochemical experiments using KCNK3-specific antibody (Toyoda et al., 2010) showed no apparent expression of KCNK3 in the developing cortex, and we did not observe compensatory up-regulation of KCNK3 expression in KCNK9 knockdown cortex (data not shown).

KCNK9 contributes to neuronal migration through the regulation of spontaneous calcium transients

How does dysfunction of KCNK9 impede migration? Our results suggest a possibility that downregulation of KCNK9 disturbed neuronal migration by increasing spontaneous calcium transients. Experiments using calcium imaging demonstrated that KCNK9 knockdown or expression of a disease-associated mutant (which behaves as a dominant-negative mutant) increased the frequency of calcium transients in migrating cortical neurons (Fig. 6). Coexpression of RNAi-insensitive KCNK9 with KCNK9 shRNA restored the pattern of calcium transients, and the migration phenotype. It is known that neuronal migration is in part regulated by neural activity and calcium signaling (Komuro and Rakic, 1998; Zheng and Poo, 2007), but activity-dependent mechanism of migration in cortical excitatory neurons has been elusive. We, as well as others, have shown that overexpression of Kir2.1 (a genetic tool to reduce neuronal excitability) in developing cortical excitatory neurons does not interfere with their migration (Cancedda et al., 2007; Mizuno et al., 2007). In the current study, we used *in utero* electroporation to express genetically-coded

calcium-sensitive indicator GCaMP3 specifically in migrating cortical neurons, and performed calcium imaging. The combination of *in utero* down-regulation of intrinsic ion channel and calcium imaging revealed that too frequent spontaneous calcium influx might impede neuronal migration in the developing cerebral cortex.

The increase of spontaneous calcium transients caused by KCNK9 knockdown is presumably mediated through depolarization of resting membrane potential as suggested by electrophysiological experiments (Fig. 5*C*). This phenotype of KCNK9 knockdown is consistent with a previous study which reported ~10mV depolarization of resting membrane potential in cerebellar granule neurons of KCNK9 knockout mice (Brickley et al., 2007). Voltage-dependent sodium and calcium channels would have more chance to open at a depolarized membrane potential. The increased calcium influx may dysregulate downstream intracellular signaling and calcium-dependent gene expression critical for the proper control of migration (Nakanishi and Okazawa, 2006).

It has been shown that blockade of calcium transients through voltage-gated calcium channels and NMDA receptors impedes the migration of cerebellar granule neurons (Komuro and Rakic, 1992; 1993). Cortical interneuron migration is also sensitive to changes in the intracellular calcium concentration that are regulated by $GABA_A$ and AMPA/NMDA receptors (Bortone and Polleux, 2009). In both types of neuron, the frequency of calcium transients positively correlates with the rate of migration, and loss of calcium transients acts as a "stop" signal for migration (Komuro and Rakic, 1996; Kumada and Komuro, 2004; Bortone and Polleux, 2009). Our results seem contradictory to these previous results, because KCNK9 knockdown induced an increase, but not a

decrease, in the frequency of calcium transients, and suppressed neuronal migration. On the other hand, our results are consistent with a previous report that showed that in immature cortical neurons, interfering with calcium transients by blocking the excitatory action of GABA enhances migration (Heck et al., 2007). Their results and ours suggest that cortical excitatory neurons may differ from cerebellar granule neurons and cortical interneurons, in that they require relatively low-levels or low frequencies of calcium transients for proper migration. Similar cell-type specific effect of calcium transients on the motility has been reported in growing axons, where the frequency of calcium transients in growth cones are inversely or directly proportional to the rate of axonal outgrowth (Gomez and Spitzer, 1999; Hutchins et al., 2011). To further clarify the relationship between calcium transients and cell motility during migration of cortical excitatory neurons, a combination of calcium and time-lapse imaging would be useful in future.

KCNK9 and developmental disorders

A dominant-negative mutant of KCNK9 (G236R) was found in patients suffering from an inherited developmental disorder, Birk Barel mental retardation dysmorphism syndrome (Barel et al., 2008). In addition, it has been reported that KCNK9 knockout mice show abnormalities in some learning tasks (Linden et al., 2007). These studies support the notion that dysfunction of KCNK9 causes a developmental disorder. We found that dysfunction of KCNK9 disrupted neuronal migration in the developing cerebral cortex. This result suggests the possibility that suppressed neuronal migration

by KCNK9 dysfunction could be a cause of mental retardation. Indeed, migration defects are closely coupled with some developmental disorders in humans (Ross and Walsh, 2001; LoTurco and Bai, 2006; Ben-Ari, 2008). For instance, microtubule-associated proteins DCX and Lis1 are responsible for cortical malformations such as subcortical band heterotopia and lissencephally, and their knockdown in an animal model disrupts neuronal migration (Bai et al., 2003; Tsai et al., 2005). Interestingly, in DCX knockdown cortex, heterotopic neurons located in the deep cortical layer and normally migrated layer II/III neurons form an abnormal neural network, and this abnormal network becomes a source of synchronous epileptogenic firings, reproducing some symptoms present in human patients (Ackman et al., 2009). We have shown that mislocated neurons, resulting from KCNK9 knockdown, stayed and slowly matured in the deep cortical layers in early postnatal period, which includes the period during which large-scale dynamic calcium transients and propagating waves have been observed in the cortex (Garaschuk et al., 2000; Khazipov and Luhmann, 2006; Allene and Cossart, 2010). Dysfunction of KCNK9 may alter the pattern of such network activities, possibly through the regulation of excitability of individual neurons or the mislocated neurons abnormally integrated into the cortical circuits.

In conclusion, we have demonstrated that KCNK potassium channels play roles in the migration of cortical excitatory neurons. KCNK potassium channels promote migration by suppressing the frequency of calcium transients to keep it within the appropriate range.

Funding

This work was supported by research grants from the Ministry of Education, Culture, Sports, Science, and Technology (MEXT) of Japan (21700350 and 23500388 to Y.T.), Grant-in-Aid for Scientific Research on Innovative Areas "Neural Diversity and Neocortical Organization" from MEXT (23123508 to Y.T.), the Global Center of Excellence program A06 to Kyoto University (T.H.), Inamori Foundation (Y.T.), Mochida Memorial Foundation (Y.T.) and Naito Foundation (Y.T.).

Acknowledgements

We thank Drs. Elizabeth Nakajima and Shin-ya Kawaguchi (Kyoto University) for critical reading of the manuscript, and Drs. Takahiko Matsuda and Constance L. Cepko (Harvard University) for a generous gift of pCAGmir30 vector.

Competing Financial Interests Statement

None

References

Ackman JB, Aniksztejn L, Crépel V, Becq H, Pellegrino C, Cardoso C, Ben-Ari Y, Represa A. 2009. Abnormal network activity in a targeted genetic model of human double cortex. J Neurosci 29:313-327.

Allene C, Cossart R. 2010. Early NMDA receptor-driven waves of activity in the developing neocortex: physiological or pathological network oscillations? J Physiol 588:83-91.

Aller MI, Wisden W. 2008. Changes in expression of some two-pore domain potassium channel genes (*KCNK*) in selected brain regions of developing mice. Neuroscience 151:1154-1172.

Arlotta P, Molyneaux BJ, Chen J, Inoue J, Kominami R, Macklis JD. 2005. Neuronal subtype-specific genes that control corticospinal motor neuron development in vivo. Neuron 45:207-221.

Bai J, Ramos RL, Ackman JB, Thomas AM, Lee RV, LoTurco JJ. 2003. RNAi reveals doublecortin is required for radial migration in rat neocortex. Nat Neurosci 6:1277-1283.

Barel O, Shalev SA, Ofir R, Cohen A, Zlotogora J, Shorer Z, Mazor G, Finer G, Khateeb S, Zilberberg N, Birk OS. 2008. Maternally inherited Birk Barel mental retardation dysmorphism syndrome caused by a mutation in the genomically imprinted potassium channel *KCNK9*. Am J Hum Genet 83:193-199.

Ben-Ari Y. 2008. Neuro-archaeology: pre-symptomatic architecture and signature of neurological disorders. Trends Neurosci 31:626-636.

Berg AP, Talley EM, Manger JP, Bayliss DA. 2004. Motoneurons express heteromeric TWIK-related acid-sensitive K+ (TASK) channels containing TASK-1 (KCNK3) and TASK-3 (KCNK9) subunits. J Neurosci 24:6693-702.

Borodinsky LN, Root CM, Cronin JA, Sann SB, Gu X, Spitzer NC. 2004. Activity-dependent homeostatic specification of transmitter expression in embryonic neurons. Nature 429:523-530.

Bortone D, Polleux F. 2009. KCC2 expression promotes the termination of cortical interneuron migration in a voltage-sensitive calcium-dependent manner. Neuron 62:53-71.

Brickley SG, Aller MI, Sandu C, Veale EL, Alder FG, Sambi H, Mathie A, Wisden W. 2007. TASK-3 two-pore domain potassium channels enable sustained high-frequency firing in cerebellar granule neurons. J Neurosci 27:9329-9340.

Cancedda L, Fiumelli H, Chen K, Poo MM. 2007. Excitatory GABA action is essential for morphological maturation of cortical neurons in vivo. J Neurosci 27:5224-5235.

Chen G, Sima J, Jin M, Wang KY, Xue XJ, Zheng W, Ding YQ, Yuan XB. 2008. Semaphorin-3A guides radial migration of cortical neurons during development. Nat Neurosci 11:36-44.

Corbo JC, Deuel TA, Long JM, LaPorte P, Tsai E, Wynshaw-Boris A, Walsh CA. 2002. Doublecortin is required in mice for lamination of the hippocampus but not the neocortex. J Neurosci. 22:7548-7557.

Day M, Carr DB, Ulrich S, Ilijic E, Tkatch T, Surmeier DJ. 2005. Dendritic excitability of mouse frontal cortex pyramidal neurons is shaped by the interaction among HCN,

Kir2, and K_{leak} channels. J Neurosci 25:8776-8787.

Deuel TA, Liu JS, Corbo JC, Yoo SY, Rorke-Adams LB, Walsh CA. 2006. Genetic interactions between doublecortin and doublecortin-like kinase in neuronal migration and axon outgrowth. Neuron 49:41-53.

Garaschuk O, Linn J, Eilers J, Konnerth A. 2000. Large-scale oscillatory calcium waves in the immature cortex. Nat Neurosci. 3:452-459.

Goldstein SA, Bockenhauer D, O'Kelly I, Zilberberg N. 2001. Potassium leak channels and the KCNK family of two-P-domain subunits. Nat Rev Neurosci 2:175-184.

Gomez TM, Spitzer NC. 1999. In vivo regulation of axon extension and pathfinding by growth-cone calcium transients. Nature 397:350-355.

Han J, Truell J, Gnatenco C, Kim D. 2002. Characterization of four types of background potassium channels in rat cerebellar granule neurons. J Physiol 542:431-444.

Hutchins BI, Li L, Kalil K. 2011. Wnt/calcium signaling mediates axon growth and guidance in the developing corpus callosum. Dev Neurobiol 71:269-283.

Heck N, Kilb W, Reiprich P, Kubota H, Furukawa T, Fukuda A, Luhmann HJ. 2007. GABA-A receptors regulate neocortical neuronal migration in vitro and in vivo. Cereb Cortex 17:138-148.

Hevner RF, Shi L, Justice N, Hsueh Y, Sheng M, Smiga S, Bulfone A, Goffinet AM, Campagnoni AT, Rubenstein JL. 2001. Tbr1 regulates differentiation of the preplate and layer6. Neuron 29:353-366.

Horikawa K, Takeichi M. 2001. Requirement of the juxtamembrane domain of the cadherin cytoplasmic tail for morphogenetic cell rearrangement during myotome

development. J Cell Biol 155:1297-1306.

Ip JP, Shi L, Chen Y, Itoh Y, Fu WY, Betz A, Yung WH, Gotoh Y, Fu AK, Ip NY. 2011. α2-chimaerin controls neuronal migration and functioning of the cerebral cortex through CRMP-2. Nat Neurosci 15:39-47.

Kang D, Han J, Talley EM, Bayliss DA, Kim D. 2004. Functional expression of TASK-1/TASK-3 heteromers in cerebellar granule cells. J Physiol 554:64-77.

Katz LC, Shatz CJ. 1996. Synaptic activity and the construction of cortical circuits. Science 274:1133-1138.

Kawaguchi SY, Hirano T. 2006. Integrin α3β1 suppresses long-term potentiation at inhibitory synapses on the cerebellar Purkinje neuron. Mol Cell Neurosci 31:416-426.

Khazipov R, Luhmann HJ. 2006. Early patterns of electrical activity in the developing cerebral cortex of humans and rodents. Trends Neurosci 29:414-418.

Koizumi H, Tanaka T, Gleeson JG. 2006. Doublecortin-like kinase functions with doublecortin to mediate fiber tract decussation and neuronal migration. Neuron. 49:55-66.

Komuro H, Rakic, P. 1992. Selective role of N-type calcium channels in neuronal migration. Science 257:806-809.

Komuro H, Rakic P. 1993. Modulation of Neuronal Migration by NMDA receptors. Science 260:95-97.

Komuro H, Rakic, P. 1996. Intracellular Ca^{2+} fluctuations modulates the rate of neuronal migration. Neuron 17:275-285.

Komuro H, Rakic, P. 1998. Orchestration of neuronal migration by activity of ion channels, neurotransmitter receptors, and intracellular Ca^{2+} fluctuations. J Neurobiol 37:110-130.

Kumada T, Komuro H. 2004. Completion of neuronal migration regulated by loss of Ca^{2+} transients. Proc Natl Acad Sci U S A 101:8479-8484.

Lauritzen I, Zanzouri M, Honoré E, Duprat F, Ehrengruber MU, Lazdunski M, Patel AJ. 2003. K^+-dependent cerebellar granule neuron apoptosis. Role of task leak K^+ channels. J Biol Chem 278:32068-32076.

Linden AM, Sandu C, Aller MI, Vekovischeva OY, Rosenberg PH, Wisden W, Korpi ER. 2007. TASK-3 knockout mice exhibit exaggerated nocturnal activity, impairments in cognitive functions, and reduced sensitivity to inhalation anesthetics. J Pharmacol Exp Ther 323:924-934.

Liu X, Hashimoto-Torii K, Torii M, Ding C, Rakic P. 2010. Gap junctions/hemichannels modulate interkinetic nuclear migration in the forebrain precursors. J Neurosci 30:4197-4209.

LoTurco JJ, Bai J. 2006. The multipolar stage and disruptions in neuronal migration. Trends Neurosci 29:407-413.

Luhmann HJ, Reiprich RA, Hanganu I, Kilb W. 2000. Cellular physiology of the neonatal rat cerebral cortex: intrinsic membrane properties, sodium and calcium currents. J Neurosci Res 62:574-584.

Manent JB, Represa A. 2007. Neurotransmitters and brain maturation: early paracrine actions of GABA and glutamate modulate neuronal migration. Neuroscientist

13:268-279.

Matsuda T, Cepko CL. 2007. Controlled expression of transgenes introduced by *in vivo* electroporation. Proc Natl Acad Sci U S A 104:1027-1032.

Meijering E, Jacob M, Sarria JC, Steiner P, Hirling H, Unser M. 2004. Design and validation of a tool for neurite tracing and analysis in fluorescence microscopy images. Cytometry A 58:167-176.

Mizuno H, Hirano T, Tagawa Y. 2007. Evidence for activity-dependent cortical wiring: formation of interhemispheric connections in neonatal mouse visual cortex requires projection neuron activity. J Neurosci 27:6760-6770.

Molyneaux BJ, Arlotta P, Menezes JR, Macklis JD. 2007. Neuronal subtype specification in the cerebral cortex. Nat Rev Neurosci 8:427-437.

Mu D, Chen L, Zhang X, See LH, Koch CM, Yen C, Tong JJ, Spiegel L, Nguyen KC, Servoss A, et al. 2003. Genomic amplification and oncogenic properties of the KCNK9 potassium channel gene. Cancer Cell 3:297-302.

Nakanishi S, Okazawa M. 2006. Membrane potential-regulated Ca^{2+} signalling in development and maturation of mammalian cerebellar granule cells. J Physiol 575:389-95.

Nieto M, Monuki ES, Tang H, Imitola J, Haubst N, Khoury SJ, Cunningham J, Gotz M, Walsh CA. 2004. Expression of Cux-1 and Cux-2 in the subventricular zone and upper layers II-IV of the cerebral cortex. J Comp Neurol 479:168-180.

Ohtsuki G., Kawaguchi S.-Y., Mishina M. & Hirano T. 2004. Enhanced inhibitory synaptic transmission in the cerebellar molecular layer of the GluRδ2 knock-out

mouse. J Neurosci 24:10900-10907 (2004)

Pei L, Wiser O, Slavin A, Mu D, Powers S, Jan LY, Hoey T. 2003. Ontogenic potential of TASK3 (Kcnk9) depends on K^+ channel function. Proc Natl Acad Sci U S A 100:7803-7807.

Picken Bahrey HL, Moody WJ. 2003. Early development of voltage-gated ion currents and firing properties in neurons of mouse cerebral cortex. J Neurophysiol 89:1761-1773.

Ross ME, Walsh CA. 2001. Human brain malformations and their lessons for neuronal migration. Annu Rev Neurosci 24:1041-1070.

Saito T, Nakatsuji N. 2001. Efficient gene transfer into the embryonic mouse brain using *in vivo* electroporation. Dev Biol 240:237-246.

Tabata H, Nakajima K. 2001. Efficient *in utero* gene transfer system to the developing mouse brain using electroporation: visualization of neuronal migration in the developing cortex. Neuroscience 103:865-872.

Tagawa Y, Kanold PO, Majdan M, Shatz CJ. 2005. Multiple periods of functional ocular dominance plasticity in mouse visual cortex. Nat Neurosci 8:380-388.

Talley EM, Solorzano G, Lei Q, Kim D, Bayliss DA. 2001. Cns distribution of members of the two-pore-domain (KCNK) potassium channel family. J Neurosci 21:7491-7505.

Tian L, Hires SA, Mao T, Huber D, Chiappe ME, Chalasani SH, Petreanu L, Akerboom J, McKinney SA, Schreiter ER, et al. 2009. Imaging neural activity in worms, flies and mice with improved GCaMP calcium indicators. Nat Methods 6:875-881.

Toyoda H, Saito M, Okazawa M, Hirao K, Sato H, Abe H, Takada K, Funabiki K,

Takada M, Kaneko T, Kang Y. 2010. Protein kinase G dynamically modulates TASK1-mediated leak K^+ currents in cholinergic neurons of the basal forebrain. J Neurosci 30:5677-5689.

Tsai JW, Chen Y, Kriegstein AR, Vallee R. 2005. LIS1 RNA interference blocks neural stem division, morphogenesis, and motility at multiple stages. J Cell Biol 170:935-945.

Watakabe A, Ichinohe N, Ohsawa S, Hashikawa T, Komatsu Y, Rockland KS, Yamamori T. 2007. Comparative analysis of layer-specific genes in mammalian neocortex. Cereb Cortex 17:1918-1933.

Weissman TA, Riquelme PA, Ivic L, Flint AC, Kriegstein AR. 2004. Calcium waves propagate through radial glial cells and modulate proliferation in the developing neocortex. Neuron 43:647-661.

Zheng JQ, Poo MM. 2007. Calcium signaling in neuronal motility. Annu Rev Cell Dev Biol 23:375-404.

Figure legends

Figure 1. ***A-C***, Expression of KCNK potassium channels during cortical development. Representative images of *in situ* hybridization showing laminar expression patterns of KCNK2 (***A***), 9 (***B***), and 10 (***C***) in the developing mouse cortex from E15 to P3. ***D***, DAPI staining shows the location of nuclei. Scale bar, 100 μm. MZ, marginal zone, CP, cortical plate, IZ, intermediate zone, SVZ, subventricular zone, VZ, ventricular zone.

Figure 2. Migration impairment caused by knockdown of KCNK potassium channels. ***A***, Immunoblotting showing the expression of KCNK channels. N-terminal EGFP-tagged KCNK channels were transfected with or without shRNA-expressing vectors in HEK293T cells. Immunoblotting of actin was performed as a loading control. ***B***, Coronal sections of P0, 3, and 5 mouse brains showing the distribution of EGFP-labeled neurons across cortical layers. Representative images of visual cortex are presented. EGFP was electroporated at E15 with control or KCNK channel shRNAs. EGFP-expressing neurons are shown in green. Arrows indicate the neurons whose migration was impaired. Scale bar, 100 μm. uCP, upper cortical plate, lCP, lower cortical plate. ***C***, Analysis of the laminar distribution of EGFP-positive neurons. Mean ± SEM is presented. **, $P < 0.01$, ***, $P < 0.001$, Dunnett test, compared with control shRNA.

Figure 3. The effects of other shRNAs targeting KCNK9 and rescue experiment. ***A***, Immunoblotting showing the expression of KCNK9. N-terminal EGFP-tagged KCNK9

were transfected with or without shRNA expressing vectors in HEK293T cells. Immunoblotting of actin was done as a loading control. ***B***, Coronal sections of P3 mouse brain. EGFP was electroporated at E15 with or without shRNAs targeting KCNK channels. Scale bar, 100 μm. ***C***, Analysis of the laminar distribution of EGFP-positive neurons. Mean ± SEM is presented. ***, $P < 0.001$, Dunnett test, compared with pSuper. ***D***, Immunoblotting showing the expression of shRNA-resistant mutant KCNK9 (KCNK9*). N-terminal EGFP-tagged KCNK9* was transfected into HEK293T cells with or without KCNK9 shRNA. Immunoblotting of actin was performed as a loading control. ***E***, Coronal cortical sections from P3 mice. KCNK9 shRNA, KCNK9 shRNA + KCNK9* (KCNK9 rescue), or KCNK9* was transfected at E15 with EGFP. ***F***, Analysis of the distribution of EGFP-positive neurons across cortical layers. Mean ± SEM is presented. ***, $P < 0.001$, Dunnett test, compared with KCNK9 shRNA. Scale bar, 100 μm.

Figure 4. Requirement for ion channel function of KCNK9 for neuronal migration. ***A***, The location of the dominant-negative mutations. ***B***, P3 coronal sections of mice transfected with EGFP or EGFP plus a dominant-negative mutant. EGFP, EGFP + G95E, or EGFP + G236R was electroporated at E15. Scale bar, 100 μm. ***C***, Laminar distribution of EGFP-positive neurons. Mean ± SEM is presented. ***, $P < 0.001$, Dunnett test, compared with EGFP. ***D***, Immunoblotting showing the expression of shRNA-resistant non-functional mutants (G95E*, G236R*). N-terminal EGFP-tagged G95E* or G236R* was transfected into HEK293T cells with or without KCNK9 shRNA.

Immunoblotting of actin was performed as a loading control. ***E***, P3 coronal sections of mice transfected with KCNK9 shRNA and an RNAi-resistant functional or non-functional KCNK9. KCNK9 shRNA + KCNK9* (KCNK9 rescue), KCNK9 shRNA + G95E*, or KCNK9 shRNA + G236R* was electroporated at E15. Scale bar, 100 μm. ***F***, Laminar distribution of EGFP-positive neurons. Mean ± SEM is presented. ***, $P < 0.001$, Dunnett test, compared with KCNK9 rescue.

Figure 5. Electrophysiological properties of migrating neurons.

A, Current changes induced by 80 ms hyperpolarizing pulses to -80 and -100 mV from the holding potential of -60 mV. ***B***, The input resistances were calculated by dividing the amplitude of voltage pulses by the amplitude of steady current. Mean ± SEM is presented. **, $P < 0.01$, Student's t-test. ***C***, Resting membrane potential recording in a current clamp condition. **, $P < 0.01$, Student's t-test. ***D***, Representative current traces induced by 80 ms depolarizing voltage pulses from -60 mV. ***E***,***F***, Current-voltage relationship of the peak inward current (***E***) and sustained outward current (***F***). Mean ± SEM is presented.

Figure 6. Spontaneous calcium transients in migrating neurons. ***A***, Representative time courses of F/F_0 recorded from control or KCNK9 shRNA-expressing migrating neurons in IZ and lower CP at P0 and 1. ***B***, The number of calcium transients during 10-min recordings. Mean ± SEM is presented. *, $P < 0.05$, **, $P < 0.01$, Student's t-test. ***C***, Representative time courses of F/F_0 recorded from control or KCNK9 shRNA, or

KCNK9 rescue-expressing migrating neurons in IZ at P1. ***D***, The number of calcium transients during 10-min recordings. Mean ± SEM is presented. *, $P < 0.05$, N.S., not significant, Dunnett test. ***E***, Representative time courses of F/F_0 recorded from control or G236R-expressing migrating neurons in IZ at P1. ***F***, The number of calcium transients during 10-min recordings. Mean ± SEM is presented. ***, $P < 0.001$, Student's t-test.

Figure 7. Immunostaining for layer-specific markers, cell division, apoptosis, and radial glia. ***A***,***B***, Confocal images of P3 coronal sections stained with Cux1, Ctip2, and Tbr1 antibodies at P3. ***A***, Images of EGFP-positive neurons expressing control shRNA in layer II/III. ***B***, Images of EGFP-positive neurons expressing KCNK9 shRNA in layer II/III, layers IV-VI, and IZ/SVZ/VZ. Arrows indicate the layer-specific marker-positive neurons, and arrowheads indicate the marker-negative neurons. ***C,E,G***, Immunostaining for markers for proliferating cells (***C***), apoptosis (***E***), and radial glia (***G***) at E17. ***C***, Immunostaining for Ki67, a marker for cells in M, G_1, S, and G_2 phases. Arrows indicate EGFP- and Ki67-double-positive cells. ***D***, Quantification of EGFP-positive proliferating cells. The fraction of proliferating cells was calculated by dividing the number of EGFP- and Ki67-double-positive cells by that of total EGFP-positive cells in 200 μm square of IZ/SVZ/VZ. ***E***, Staining of apoptotic cells with TUNEL method. Arrows indicate TUNEL-positive cells. ***F***, Quantification of apoptotic cells. The number of TUNEL-positive cells was counted in 200 μm square of IZ/SVZ/VZ. ***G***, Immunostaining for Nestin, a marker for radial glia. The structure of radial glial

scaffold was not altered by knockdown of KCNK9. Scale bar, ***A*-*C*,*E***, 100 μm. ***G***, 50 μm.

Figure 8. Morphological development of mislocated neurons. ***A***, Coronal sections of P10, 15, and 35 mouse brain transfected with KCNK9 shRNA at E15. Scale bar, 100 μm. ***B***, Laminar distribution of EGFP-positive neurons from P10 to P35. Mean ± SEM is presented. *, $P < 0.05$, Dunnett test, compared with P10. ***C*-*E***, Confocal images of mislocated neurons during development (upper panel). Scale bar, 100 μm. Dendritic morphology of the mislocated neurons reconstructed with NeuronJ (lower panel). Scale bar, 200 μm. ***F***, ***G***, Developmental changes of branch points (***F***) and total length (***G***) of dendrites of mislocated neurons. Mean ± SEM is presented. *: $P < 0.05$, ***: $P < 0.001$, Dunnett test, compared with P10.

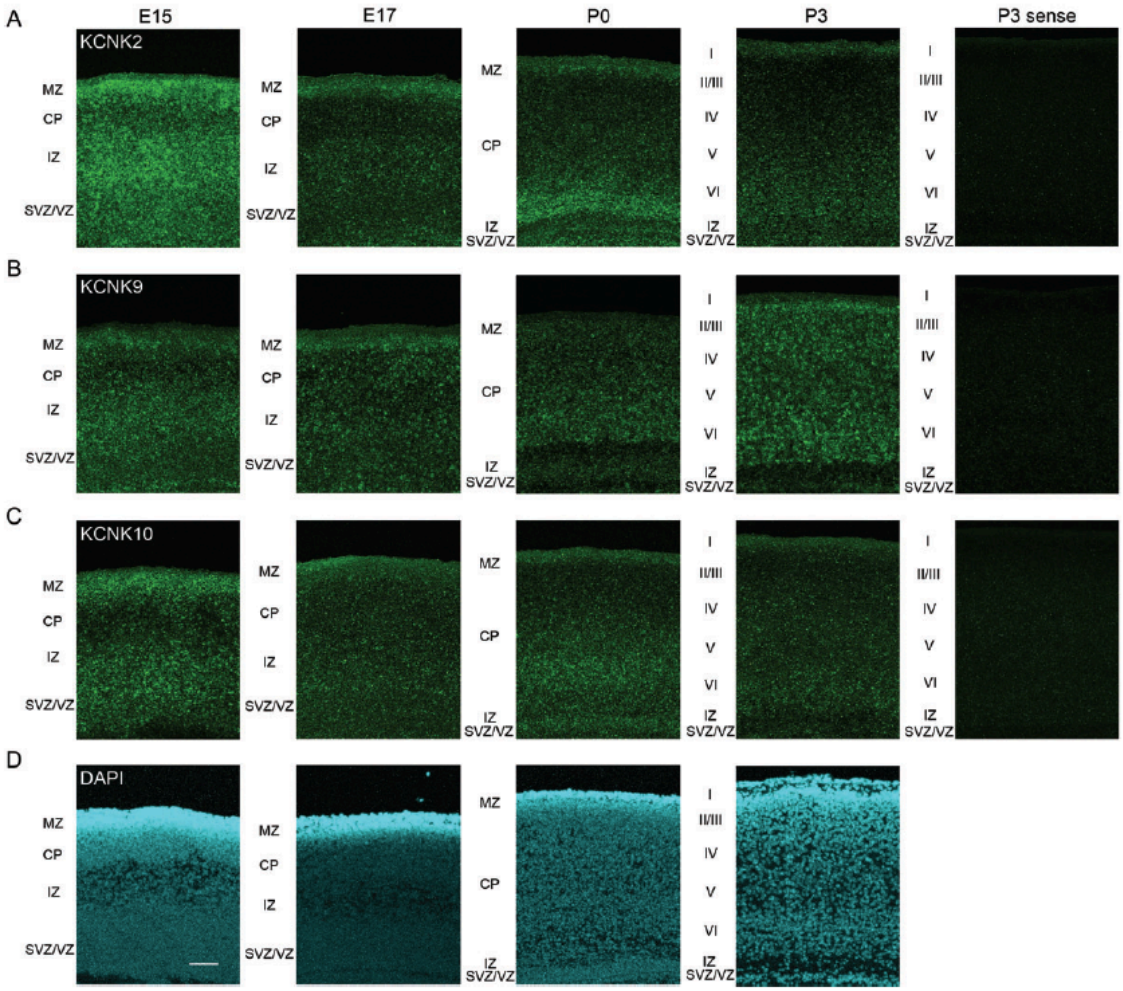
A
E15
E17
P0
P3
P3 sense
KCNK2
B
KCNK9
C
KCNK10
D
DAPI
MZ
CP
IZ
SVZ/VZ
I
II/III
IV
V
VI

Figure 1

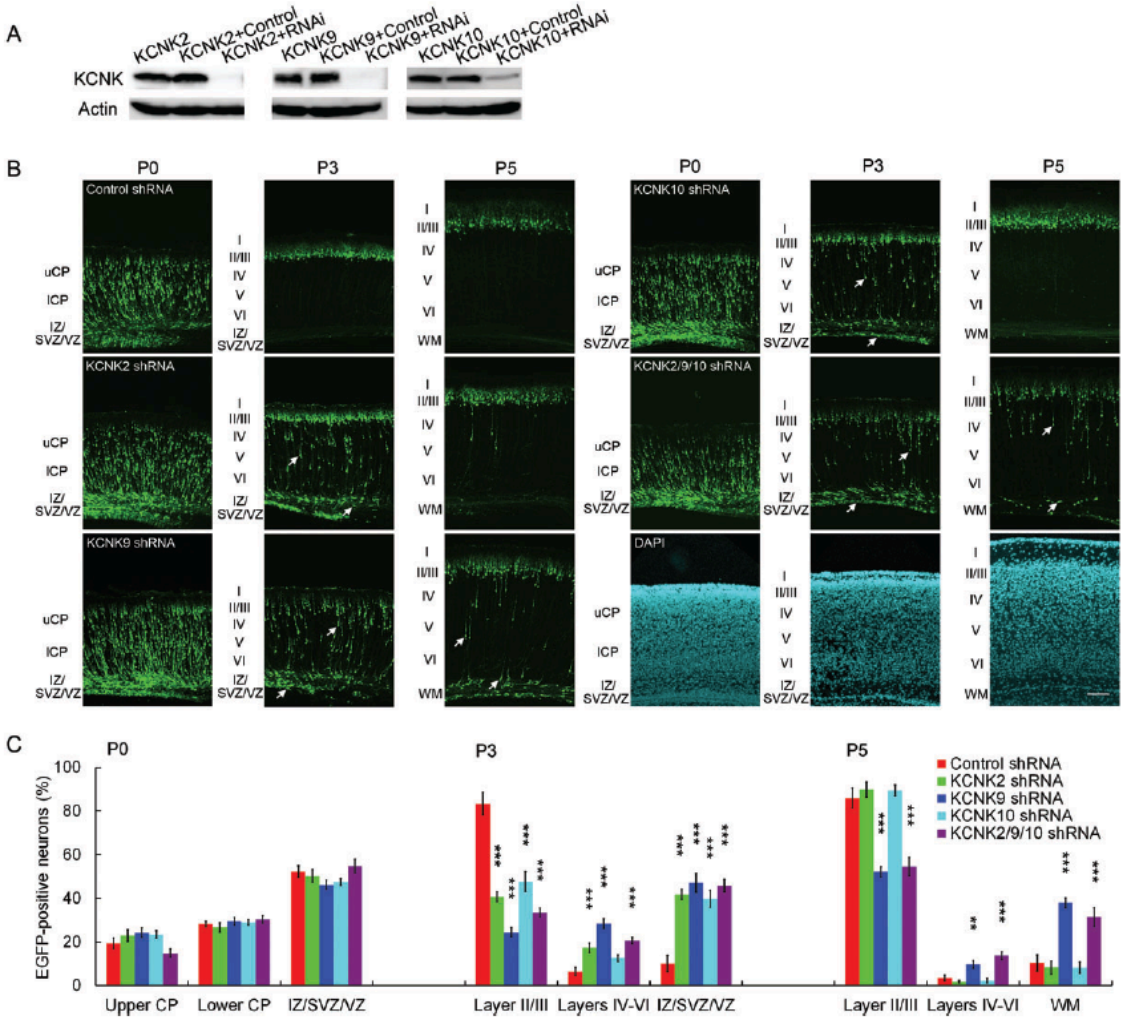
A
KCNK2
KCNK2+Control
KCNK2+RNAi
KCNK9
KCNK9+Control
KCNK9+RNAi
KCNK10
KCNK10+Control
KCNK10+RNAi
KCNK
Actin
B
P0
P3
P5
Control shRNA
KCNK10 shRNA
KCNK2 shRNA
KCNK2/9/10 shRNA
KCNK9 shRNA
DAPI
uCP
lCP
IZ/SVZ/VZ
I
II/III
IV
V
VI
WM
C
EGFP-positive neurons (%)
Control shRNA
KCNK2 shRNA
KCNK9 shRNA
KCNK10 shRNA
KCNK2/9/10 shRNA
Upper CP
Lower CP
IZ/SVZ/VZ
Layer II/III
Layers IV-VI
WM

Figure 2

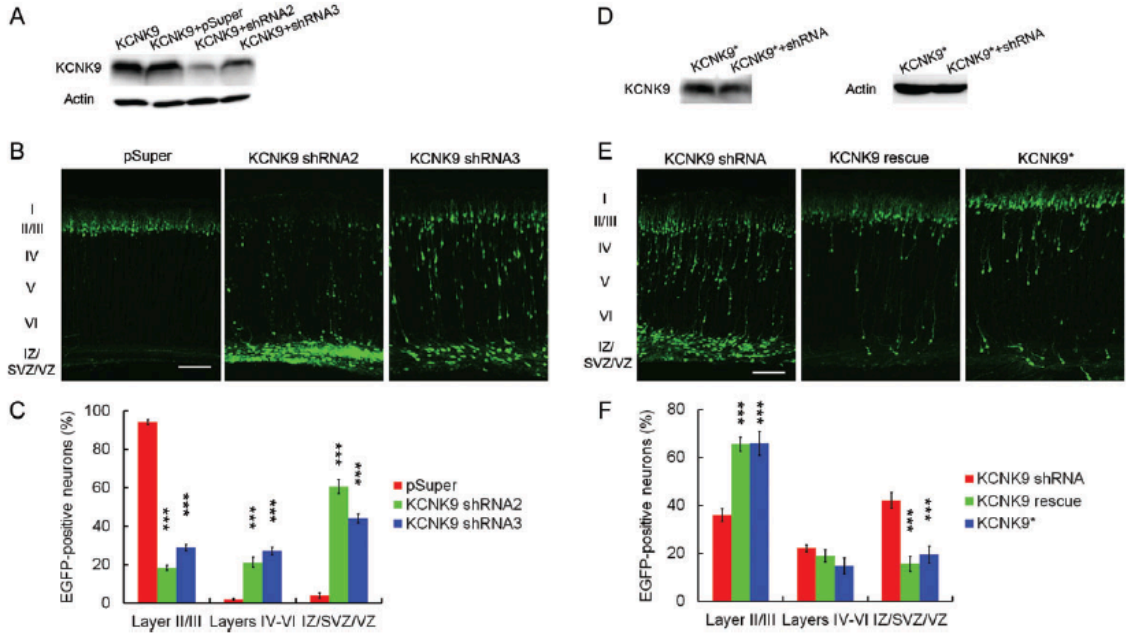
A
KCNK9
KCNK9+pSuper
KCNK9+shRNA2
KCNK9+shRNA3
KCNK9
Actin
D
KCNK9*
KCNK9*+shRNA
KCNK9
KCNK9*
KCNK9*+shRNA
Actin
B
pSuper
KCNK9 shRNA2
KCNK9 shRNA3
I
II/III
IV
V
VI
IZ/
SVZ/VZ
E
KCNK9 shRNA
KCNK9 rescue
KCNK9*
C
EGFP-positive neurons (%)
100
80
60
40
20
0
***
pSuper
KCNK9 shRNA2
KCNK9 shRNA3
Layer II/III
Layers IV-VI
IZ/SVZ/VZ
F
80
60
40
20
0
KCNK9 shRNA
KCNK9 rescue
KCNK9*

Figure 3

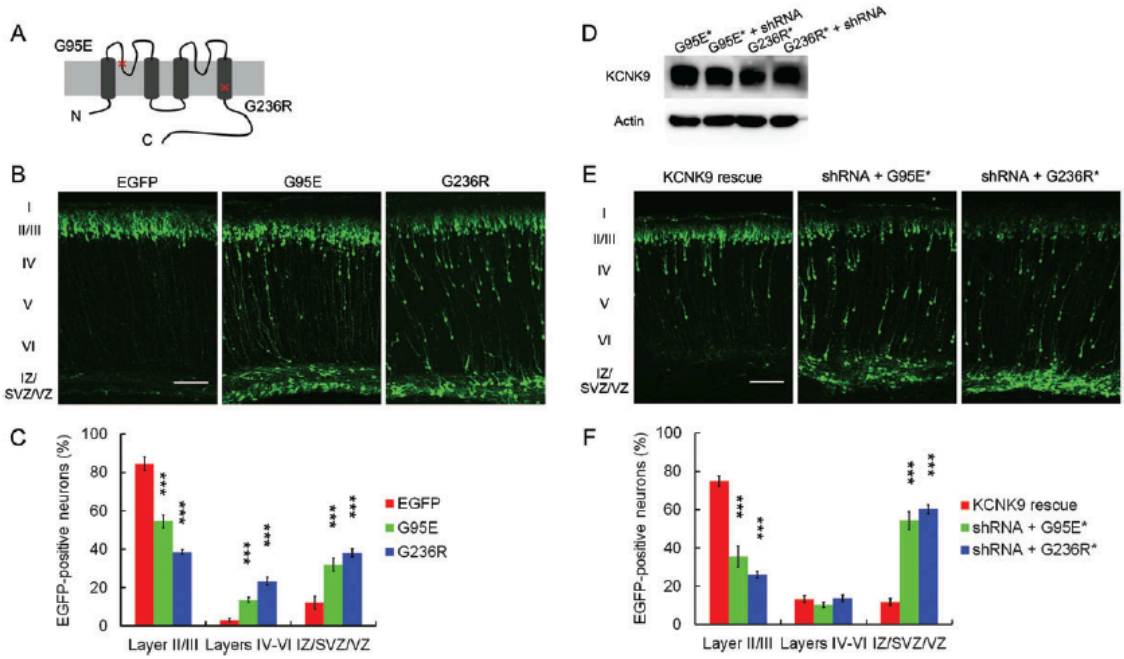
A
G95E
G236R
N
C
D
G95E*
G95E* + shRNA
G236R*
G236R* + shRNA
KCNK9
Actin
B
EGFP
G95E
G236R
I
II/III
IV
V
VI
IZ/
SVZ/VZ
E
KCNK9 rescue
shRNA + G95E*
shRNA + G236R*
C
EGFP-positive neurons (%)
100
80
60
40
20
0
***
EGFP
G95E
G236R
Layer II/III
Layers IV-VI
IZ/SVZ/VZ
F
KCNK9 rescue
shRNA + G95E*
shRNA + G236R*

Figure 4

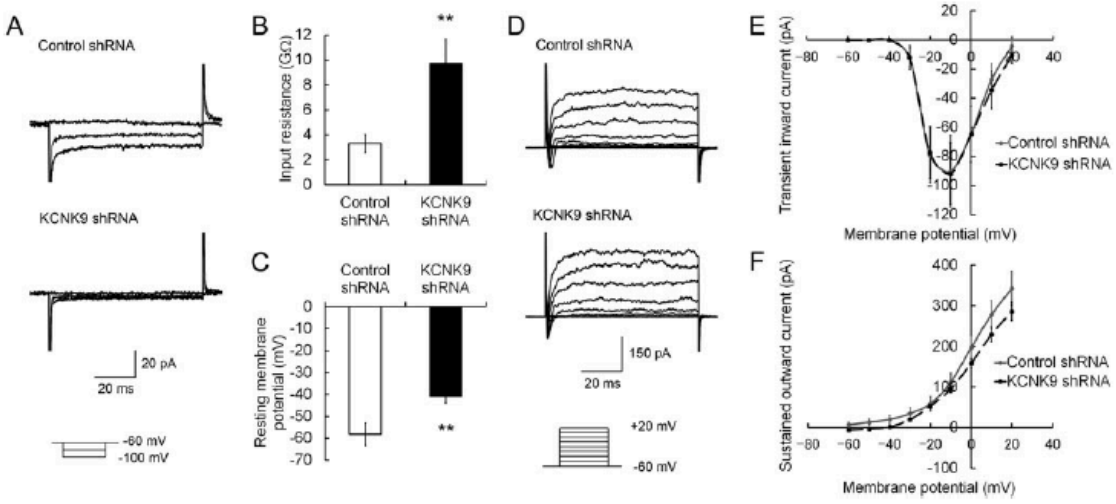
A
Control shRNA
KCNK9 shRNA
20 pA
20 ms
-60 mV
-100 mV
B
Input resistance (GΩ)
Control shRNA
KCNK9 shRNA
**
C
Resting membrane potential (mV)
Control shRNA
KCNK9 shRNA
**
D
Control shRNA
KCNK9 shRNA
150 pA
20 ms
+20 mV
-60 mV
E
Transient inward current (pA)
Membrane potential (mV)
Control shRNA
KCNK9 shRNA
F
Sustained outward current (pA)
Membrane potential (mV)
Control shRNA
KCNK9 shRNA

Figure 5

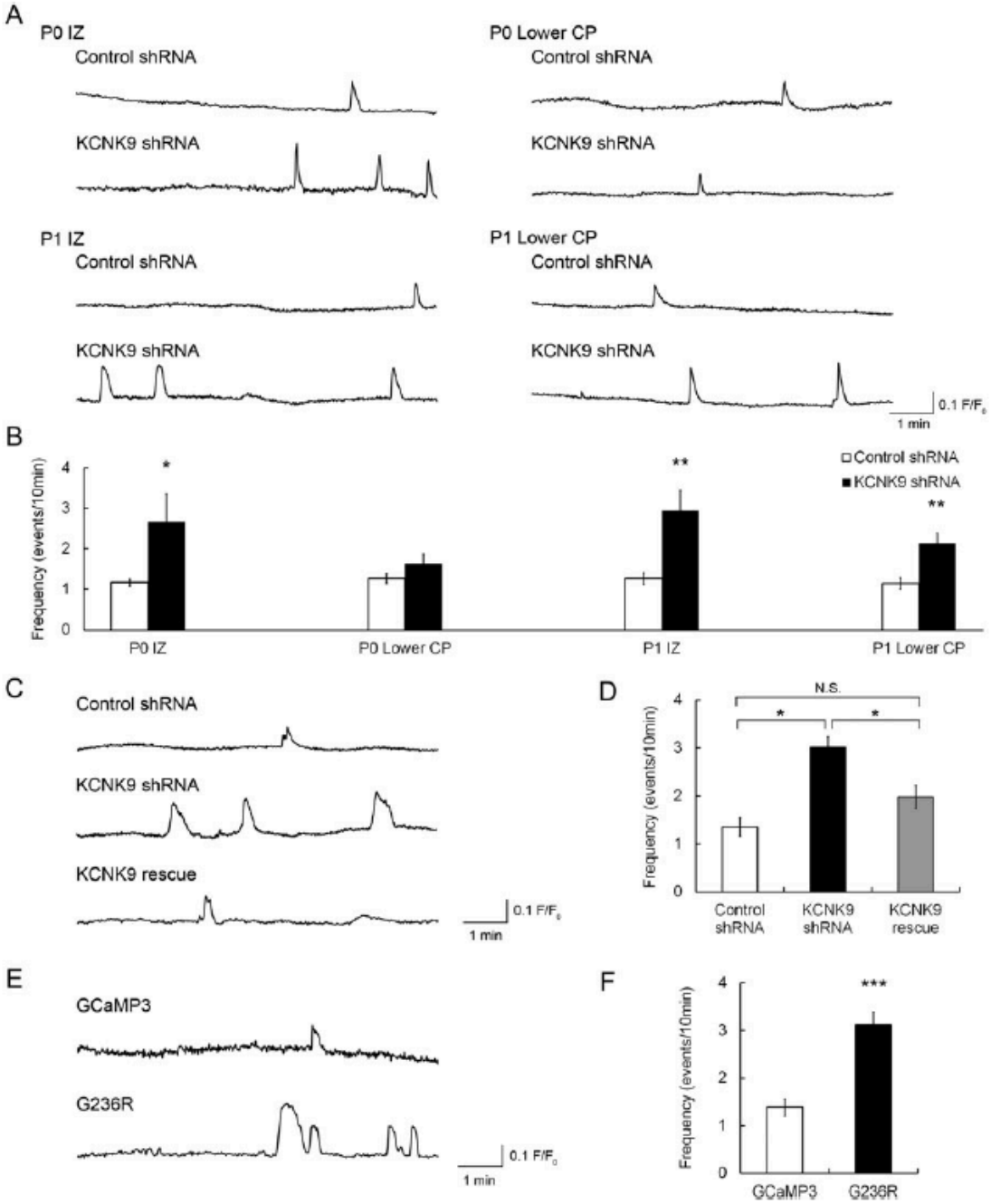
A
P0 IZ
Control shRNA
KCNK9 shRNA
P0 Lower CP
Control shRNA
KCNK9 shRNA
P1 IZ
Control shRNA
KCNK9 shRNA
P1 Lower CP
Control shRNA
KCNK9 shRNA
0.1 F/F0
1 min
B
Frequency (events/10min)
Control shRNA
KCNK9 shRNA
P0 IZ
P0 Lower CP
P1 IZ
P1 Lower CP
C
Control shRNA
KCNK9 shRNA
KCNK9 rescue
0.1 F/F0
1 min
D
N.S.
Frequency (events/10min)
Control shRNA
KCNK9 shRNA
KCNK9 rescue
E
GCaMP3
G236R
0.1 F/F0
1 min
F
Frequency (events/10min)
GCaMP3
G236R

Figure 6

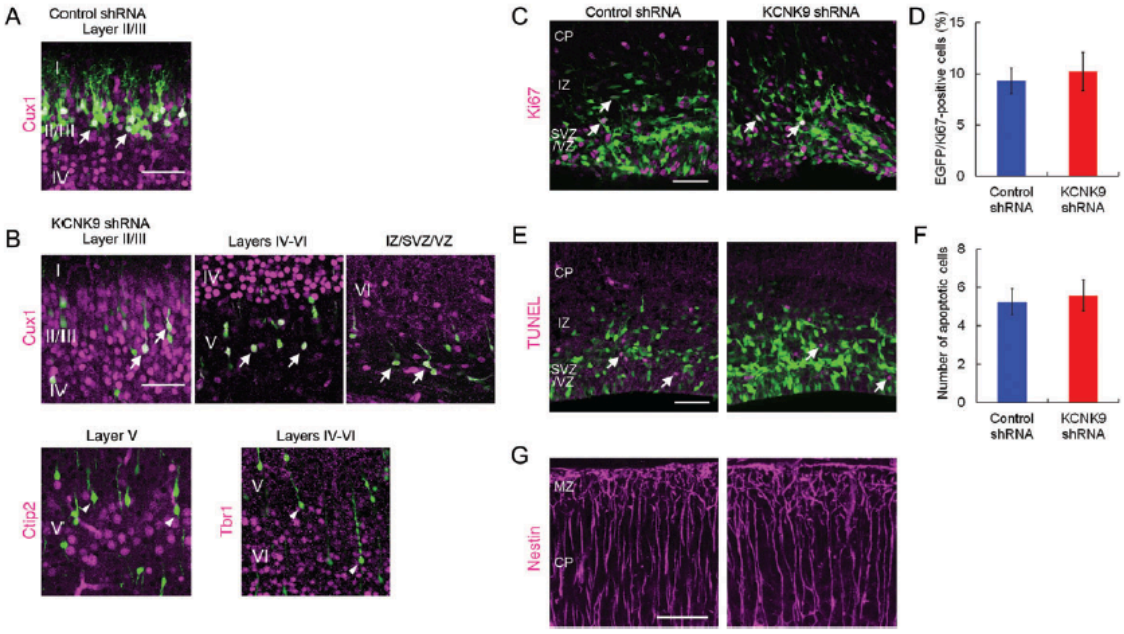
A
Control shRNA
Layer II/III
Cux1
I
II/III
IV
B
KCNK9 shRNA
Layer II/III
Layers IV-VI
IZ/SVZ/VZ
Cux1
Clip2
Layer V
Layers IV-VI
Tbr1
C
Control shRNA
KCNK9 shRNA
Ki67
CP
IZ
SVZ
VZ
D
EGFP/Ki67-positive cells (%)
Control shRNA
KCNK9 shRNA
E
TUNEL
F
Number of apoptotic cells
G
Nestin
MZ
CP

Figure 7

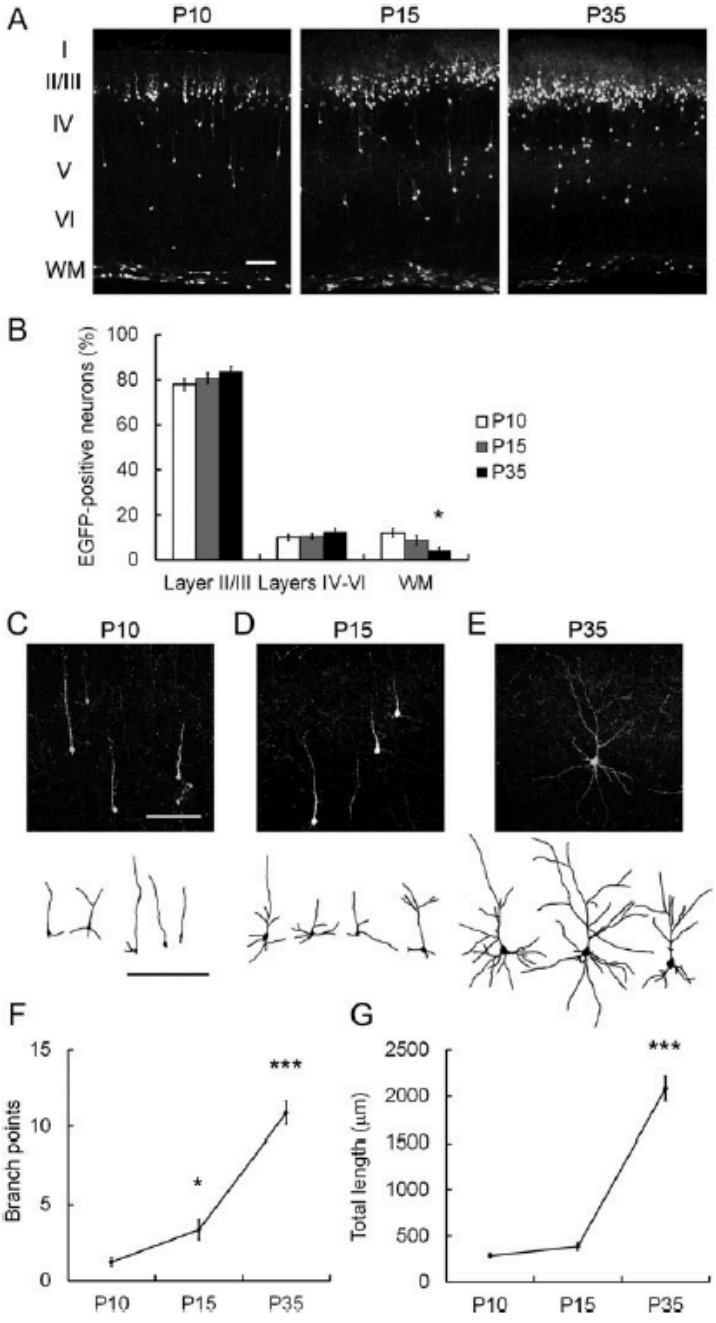
A
P10
P15
P35
I
II/III
IV
V
VI
WM
B
EGFP-positive neurons (%)
100
80
60
40
20
0
P10
P15
P35
*
Layer II/III
Layers IV-VI
WM
C
P10
D
P15
E
P35
F
Branch points
15
10
5
0
***
*
P10
P15
P35
G
Total length (µm)
2500
2000
1500
1000
500
0
***
P10
P15
P35

Figure 8

Supplementary Table1. Sequences of KCNK channel shRNAs.

Construct	Sequence
Control shRNA	5' CTCCTCAATCGTTAGATGA 3'
KCNK2 shRNA	5' GGCCATTAATGTTATGAAA 3'
KCNK9 shRNA	5' CTGCTGAAACGTATCAAGA 3'
KCNK10 shRNA	5' CAAACAGTTATGAAGTGGA 3'
KCNK9 shRNA2	5' GCGAGGAGGAGAAACTTAA 3'
KCNK9 shRNA3	5' GTCTCAGAGGCAAGTACAA 3'

Red letters indicate mutated bases of KCNK9 shRNA.

Supplementary Table 2. Summary of analysis of neuronal migration.

Age	Contstruct	Fraction of neurons (%) (P value (Dunnett test))			n
		Upper CP or Layer II/III	Lower CP or Layers IV-VI	IZ/SVZ/VZ or WM	
P0	Control shRNA	19.4 ± 2.5	28.3 ± 1.2	52.3 ± 2.7	12
	KCNK2 shRNA	23.0 ± 2.7 (0.630)	26.7 ± 2.2 (0.905)	50.3 ± 3.0 (0.955)	11
	KCNK9 shRNA	24.3 ± 2.1 (0.356)	29.5 ± 1.7 (0.964)	46.2 ± 2.1 (0.310)	11
	KCNK10 shRNA	23.5 ± 1.8 (0.503)	29.0 ± 1.2 (0.992)	47.5 ± 1.5 (0.495)	12
	KCNK2/9/10 shRNA	14.8 ± 2.0 (0.378)	30.4 ± 1.6 (0.756)	54.8 ± 3.2 (0.895)	13
P3	Control shRNA	83.4 ± 5.1	6.5 ± 1.9	10.1 ± 3.6	11
	KCNK2 shRNA	40.7 ± 2.3 (< 0.001)	17.4 ± 2.1 (< 0.001)	41.9 ± 2.3 (< 0.001)	11
	KCNK9 shRNA	24.5 ± 2.1 (< 0.001)	28.4 ± 2.3 (< 0.001)	47.1 ± 4.3 (< 0.001)	10
	KCNK10 shRNA	47.7 ± 4.5 (< 0.001)	12.6 ± 1.5 (0.081)	39.8 ± 3.8 (< 0.001)	11
	KCNK2/9/10 shRNA	33.5 ± 2.1 (< 0.001)	20.7 ± 1.5 (< 0.001)	45.9 ± 3.0 (< 0.001)	14
P5	Control shRNA	86.0 ± 4.6	3.6 ± 1.3	10.4 ± 3.7	14
	KCNK2 shRNA	89.9 ± 3.5 (0.872)	1.9 ± 0.6 (0.698)	8.3 ± 3.1 (0.977)	12
	KCNK9 shRNA	52.2 ± 2.4 (< 0.001)	9.8 ± 1.8 (0.002)	38.0 ± 2.3 (< 0.001)	10
	KCNK10 shRNA	89.5 ± 2.6 (0.906)	2.3 ± 1.1 (0.858)	8.2 ± 2.7 (0.975)	12
	KCNK2/9/10 shRNA	54.8 ± 4.2 (< 0.001)	13.8 ± 1.7 (< 0.001)	31.5 ± 4.4 (< 0.001)	14
P3	pSuper	94.1 ± 1.3	2.0 ± 0.3	3.9 ± 1.3	12
	KCNK9 shRNA2	18.3 ± 1.4 (< 0.001)	21.1 ± 2.6 (< 0.001)	60.6 ± 3.6 (< 0.001)	11
	KCNK9 shRNA3	28.8 ± 1.6 (< 0.001)	27.1 ± 1.9 (< 0.001)	44.1 ± 2.3 (< 0.001)	11
P3	KCNK9 shRNA	35.9 ± 2.7	22.1 ± 1.4	42.0 ± 3.3	11
	KCNK9 rescue	65.4 ± 3.0 (< 0.001)	18.9 ± 2.5 (0.583)	15.6 ± 3.1 (< 0.001)	11
	KCNK9*	65.8 ± 4.9 (< 0.001)	14.7 ± 3.3 (0.085)	19.4 ± 3.6 (< 0.001)	11
P3	EGFP	84.6 ± 3.6	3.2 ± 0.9	12.2 ± 3.3	10
	G95E	54.6 ± 3.4 (< 0.001)	13.5 ± 1.4 (< 0.001)	31.9 ± 3.4 (< 0.001)	12
	G236R	38.5 ± 1.1 (< 0.001)	23.3 ± 2.0 (< 0.001)	38.1 ± 2.1 (< 0.001)	11
P3	KCNK9 rescue	74.9 ± 2.7	13.3 ± 1.8	11.8 ± 1.9	13
	shRNA + G95E*	35.4 ± 5.4 (< 0.001)	10.3 ± 1.3 (0.353)	54.3 ± 4.6 (< 0.001)	12
	shRNA + G236R*	26.0 ± 1.7 (< 0.001)	13.7 ± 1.7 (0.982)	60.3 ± 2.3 (< 0.001)	12
P10	KCNK9 shRNA	77.9 ± 2.7	10.0 ± 1.4	12.1 ± 1.8	11
P15		80.7 ± 2.4 (0.635)	10.6 ± 1.1 (0.926)	8.7 ± 2.0 (0.322)	15
P35		83.6 ± 2.4 (0.243)	12.6 ± 1.3 (0.291)	4.1 ± 1.3 (0.014)	10

N indicates the number of sections analyzed (one per mouse).

Supplementary Table 3. Sequences of primers for cloning of KCNK channels.

Construct	Direction	Sequence
KCNK9	forward	5' GGGAATTCACCATGAAGCGGCAGAACGTGC 3'
	reverse	5' CCGGATCCTTAGATGGACTTGCGACGGAGG 3'
KCNK9*	forward	5' GGGAATTCACCATGAAGCGGCAGAACGTGC 3'
	mutation reverse	5' AATTCTCTTTAATAAGTAGCGCACGAAGGT 3'
	mutation forward	5' TTATTAAAGAGAATTAAAAAGTGCTGTGGC 3'
	reverse	5' CCGGATCCTTAGATGGACTTGCGACGGAGG 3'
KCNK9 G95E	forward	5' GGGAATTCACCATGAAGCGGCAGAACGTGC 3'
	mutation reverse	5' CAGTTCCAGGTGCAGCATGTCCATATTCGA 3'
	mutation forward	5' TCGAATATGGACATGCTGCACCTGGAACTG 3'
	reverse	5' CCGGATCCTTAGATGGACTTGCGACGGAGG 3'
KCNK9 G236R	forward	5' GGGAATTCACCATGAAGCGGCAGAACGTGC 3'
	mutation reverse	5' ATTGAGGAAGGCACGGATGACGGTCAGGCC 3'
	mutation forward	5' GGCCTGACCGTCATCCGTGCCTTCCTCAAT 3'
	reverse	5' CCGGATCCTTAGATGGACTTGCGACGGAGG 3'
EGFP-KCNK9	EGFP forward	5' CAGAATTCGCCACCATGGTGAGCAAGGGCG 3'
	fusion reverse	5' TGCCGCTTCATTGCAGATCCCTTGTACAGC 3'
	fusion forward	5' GCTGTACAAGGGATCTGCAATGAAGCGGCA 3'
	KCNK9 reverse	5' CCGGATCCTTAGATGGACTTGCGACGGAGG 3'
EGFP-KCNK2	EGFP forward	5' CCAAGCTTGCCACCATGGTGAGCAAGGGCG 3'
	fusion reverse	5' GGGGCCGCCATTGCAGATCCCTTGTACAGC 3'
	fusion forward	5' GCTGTACAAGGGATCTGCAATGGCGGCCCC 3'
	KCNK2 reverse	5' CTCGAGCTACTTCATGTTCTCAATGACAGC 3'
EGFP-KCNK10	EGFP forward	5' CCAAGCTTGCCACCATGGTGAGCAAGGGCG 3'
	fusion reverse	5' GAAAAATACATTGCAGATCCCTTGTACAGC 3'
	fusion forward	5' GCTGTACAAGGGATCTGCAATGTATTTTTC 3'
	KCNK10 reverse	5' CTGTCGACTTAGTTTCTGTCTTCAAGTAAA 3'